JURNAL POLIMESIN
Unit Penelitian dan Pengabdian Kepada Masyarakat (P2M)
Politeknik Negeri Lhokseumawe
ISSN Print: 1693-5462, ISSN Online: 2549-1199
Website: http://e-jurnal.pnl.ac.id/index.php/polimesin

Experimental and Simulation Evaluation of Temperature and Air Flow in Tunnel-Type Dryers: Preliminary Study

Akhyar[1], Darwin Harun[1], Muhammad Robby[1], Muhammad Ilham Maulana[1], Ahmad Farhan[2]
[1]Program Studi Teknik Mesin, Fakultas Teknik, Universitas Syiah Kuala.
Banda Aceh. 23111. Indonesia
[2]Program Studi Fisika, FKIP, Universitas Syiah Kuala.
Banda Aceh. 23111. Indonesia.
[*]**Email:** akhyar@unsyiah.ac.id

Abstract

Solar energy is a source of electricity for various industrial applications, such as water heating and drying. In the drying application, energy is transferred from one point to another due to the temperature difference of the sample material. This promoted the significant use of dryers by both farmers and fishermen to preserve their harvest or catch. However, there are several problems associated with the open system drying, such as inconsistent drying duration, dirt, fungus contamination, and rain. Therefore, this research aims to analyze heat transfer and airflow in the drying chamber of a tunnel-type application, using experimental and computational simulations. The general applied methods encompassed measuring the dryer's in situ temperature, modeling the heat transfer, and analyzing the computational fluid dynamics(CFD) simulations for the airflow in the drying chamber between 08:00-15:30 GMT+7 (February 9, 2021). The temperature and airflow simulations of the system were analyzed and validated without a load of dried materials. Based on the measurement results, the minimum inlet and outlet temperatures occurred at 30.2ºC (08.00 GMT+7) and 24ºC, similar to the simulation at 31.2ºC (08:00 GMT+7). Meanwhile, the maximum inlet and outlet temperatures were evaluated at 45.7 and 39ºC, with an outlet simulation temperature of 41.5ºC (12:00 GMT+7). These overall results indicated that the temperature values did not vary extensively. Therefore, the applied drying system is best suitable for post-harvest agricultural, forestry, and marine drying applications.
Keywords: temperature analysis, airflow, computational fluid dynamics, tunnel-type dryer.

1. Introduction

Solar energy serves as a means of electricity supply without depletion. This high sustainability resource plays a fundamental role as a substitute for fossil fuels to further transition from carbon to green technology. Several preliminary studies have been conducted on solar applications, particularly in the form of space heating, hot water supply, electricity, drying technology [1], heating devices, water desalination, air conditioning and cooling, power generation [2], stoves [3] [4-6], etc. According to these studies, one of the major disadvantages of solar applications is the intermittent nature, where an energy storage system is needed [7]. Indonesia's daily average solar intensity occurs at approximately 4.8 kWh/m^2 [8].

Fishers typically use solar energy utilization in Ache province for post-harvest activities, such as drying, which aids in its economic development. This region geographically has a coastline of 1,660 km, with approximately 295,370 km^2 of marine waters and an exclusive economic zone (EEZ) of 238,807 km^2. Furthermore, it is surrounded by territorial, archipelagic, and EEZ waters of 220,090 tons, 203,320 tons, and ± 432,410 tons [9].

Aceh farmers are generally faced with difficulty predicting total harvests, thereby leading to a rapid decline in prices and product spoilage. This led to the use of the drying process, which is among the oldest means of food preservation carried out in the open. There are several advantages associated with solar energy as a drying heat source, such as its affordability and abundance in nature. Irrespective of these advantages, there are also some disadvantages of using the open drying method, such as its dependence on weather. Therefore, using energy sources from burning fuel provides a suitable alternative [10].

One of the most common types of solar dryers is rotary, which comprises a cylindrical sleeve capable of rotating horizontally or tilting downward. The sample material enters from one end of the cylinder while the dried product exits from the other terminal [11]. Another type is the tower dryer, which contains a series of circular trays mounted in a row upon a rotating central axis. The dry material moves in the heating cavity [12], while the screw conveyor is an indirect continuous heat dryer [13]. Meanwhile, the sample material is slowly transported over the metal along a drying tunnel fanned by hot air [14]. These various brands of solar dryers are employed in large-scale industrial applications. However, a simple and effective application is needed for an easy and complete drying process. This research aims to obtain the characteristics of heat transfer and airflow in the constructed tunnel-type drying chamber. These attributes were analyzed by computational simulations, while the experimental temperature measurements were also performed on the dryer to validate the simulation results.

This initial test examines the performance and suitability of the designed and built dryer for post-harvest utilization.

2. Method

2.1. Tunnel Type Dryer Design

Figure 1 shows the design and size of the tunnel-type dryer constructed at the Fluid Mechanics Laboratory, Department of Mechanical and Industrial Engineering, Syiah Kuala University, Banda Aceh, Indonesia. The dryer was easily manufactured with movable parts suitable for subsequent applications. In general, the tunnel-type construction is divided into several rooms with length, width, and height of 794 x 200 x 120 cm.

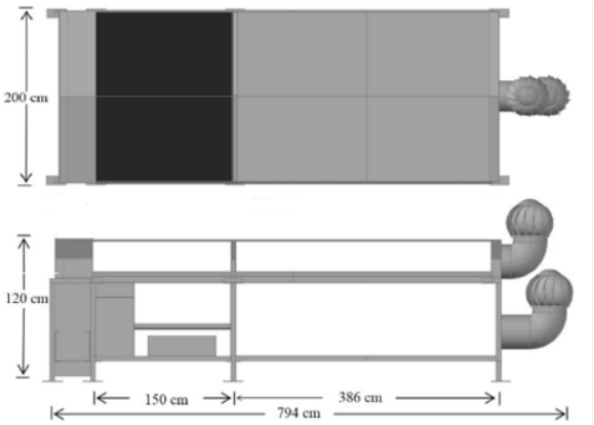

Figure 1: Tunnel type dryer design and size [15].

The solar collector plate helps absorb sunlight for the drying process, while another component stores and converts into heat, which is used to increase the air temperature in the chamber. However, not all light emissions are absorbed, as certain quantities are also reflected. The solar collector material consists of an aluminum metal alloy, which is readily available. Its surface is coated with black paint to increase the absorbing ability of heat energy from sunlight. This component also raises the air temperature in the dryer tunnel. The drying column is a chamber designed like a tunnel with the sample material commonly placed on its plate. In addition, its mainframe comprises wood and a steel frame, while unpainted aluminum plates are attached to the walls as the tunnel-type casing.

2.2. Basic Equations

The three basic equations derived from the conservation laws of mass and energy are mass, momentum, and energy conservation. These laws led to the evolution of the Navier-Stokes and the energy equations [16]. The Reynolds number in this simulation appeared above 2000, leading to a turbulent airflow pattern in the drying chamber [17]. Numerous turbulent models are embedded in commercial computational fluid dynamics (CFD) codes, where their applications are easily adapted to inherent cases [16]. A typical example is the standard k-ε model often applied in industry-standard drying processes [18,19]. This semi-empirical model is based on the transport model equations, including the turbulent kinetic energy (k) and its dissipation rate (ε). The transport value for k is derived from the exact equation, using physical reasoning with minimal resemblance to its mathematical partner [20]. Furthermore, the turbulent kinetic energy (k), and its dissipation rate (ε) are obtained from the following transport equations:

$$\frac{\partial}{\partial t}(\rho k)+\frac{\partial}{\partial x_i}(\rho k u_i)=\frac{\partial}{\partial x_j}\left[\left(\mu+\frac{\mu_t}{\sigma_k}\right)\frac{\partial k}{\partial x_j}\right]+G_k+G_b-\rho\varepsilon-Y_M+S_k \quad (1)$$

$$\frac{\partial}{\partial t}(\rho \varepsilon)+\frac{\partial}{\partial x_i}(\rho \varepsilon u_i)=\frac{\partial}{\partial x_j}\left[\left(\mu+\frac{\mu_t}{\sigma_\varepsilon}\right)\frac{\partial \varepsilon}{\partial x_j}\right]+C_{1\varepsilon}\frac{\varepsilon}{k}(G_k+G_{3\varepsilon}G_b)-C_{2\varepsilon}\rho\frac{\varepsilon^2}{k}+S_\varepsilon \quad (2)$$

The convection heat and mass transfer modeling in the k- ε model is given by the following equation [20]:

$$\frac{\partial}{\partial t}(\rho E)+\frac{\partial}{\partial x_i}[U_i(\rho E+p)]=\frac{\partial}{\partial x_j}\left[\left(k+\frac{C_p\mu_t}{Pr_t}\right)\frac{\partial T}{\partial x_i}+U_i(\tau_{ij})_{eff}\right]+S_h \quad (3)$$

2.3. Experiment and Simulation Parameters

This research provides a preliminary approach to manufacturing a drying chamber using computational simulations tools with appropriate temperature and airflow. The simulations and experiments occurred under no-load or dry material conditions. Air circulation in this tunnel-type dryer was observed using computational field dynamics (CFD). The turbine ventilator installed at the tunnel terminal forces hot air containing moisture from the sample material to exit through the outlet. However, this process is usually conducted at a low acceleration because the shaft rotates on the turbine fins. A type K thermocouple cable was used to collect temperature data connected directly to the monitor. The temperature reading from the measuring instrument was recorded every 30 minutes, and the locations were the inlet in the drying chamber, namely T1, T2, and T3, as well as the outlet. These measurements were obtained on February 9, 2021, at the Faculty of Engineering

field, Syiah Kuala University, Banda Aceh, Aceh province, Indonesia.

The simulation process started by building a 3D model of the tunnel-type dryer before importing it into the Ansys application for further meshing, as shown in Figure 2. This was followed by identifying the boundary plane in the geometry, commonly referred to as name selection. Figure 3 represents the identified areas of the dryer as the inlet, outlet, wall, and floor.

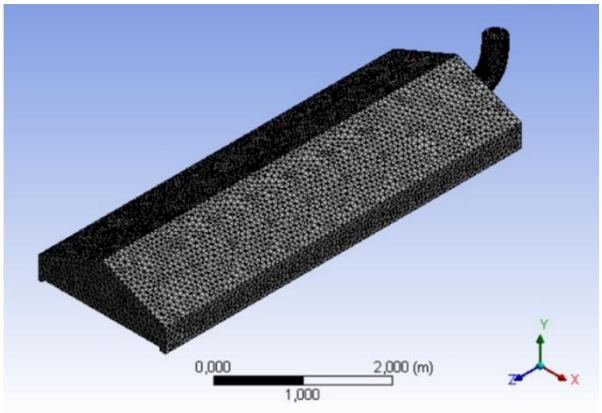

Figure 2: Meshing geometry on the dryer.

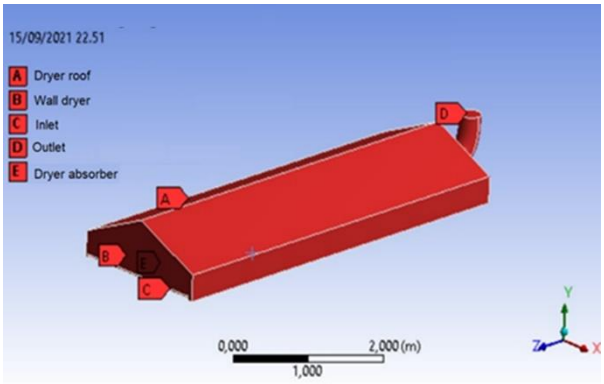

Figure 3: The naming process on the tunnel-type dryer system.

The input data parameters of the dryer consist of the pressure-based scale type (mm) and steady time. Meanwhile, the corresponding model data were energy equation (on) and K-omega viscous model comprising K-omega, SST, and options production limiter. Others include radiation, such as Rosseland, and Solar loading with a degree and deg latitude of 95.32375 and 5.54829. The Time Zone was+- 7 GMT, while the north and east mesh orientations were 1 and -1 for February 2021. In addition, the input material data were the fluid for air, solid for aluminum, and HDPE.

The input boundary conditions were reference frame solute, coordinate system, Cartesian (XY Z), and inlet temperature of 30.2, 32.8, 42.3, 44.3, 45.3, 44.8, and 41.5ºC. The selected air velocity, aluminum density, and specific heat were obtained at 3 m^{-1}, 2,710 kg/m^3, and 897 J/kg-k. Meanwhile, the boundary condition for the input outlet occurred as a pressure-outlet by default.

The roof was selected as HDPE with a heat transfer coefficient, density, and specific heat capacity of 6.87 w/m^2-k, 940 kg/m3, and 1330 J/kg-K. This was followed by determining the thermal condition at temperatures of 26, 29, 30, 32, 32, 32, 30, and 31º. Radiation was observed in the solar ray tracing (semi-transparent) using high-density polyethylene with a wall thickness of 0.002m. Furthermore, the input data for the floor and walls include thermal conditions, such as heat transfer coefficient of 6.87 w/m^2-k and free stream temperature of 26, 29, 30, 32, 32, 32, 30, and 31^0. Radiation was also involved in the solar ray tracing using aluminum with a wall thickness of 0.004 m.

3. Results and Discussion

3.1. Experimental

Figure 4 indicates the data recording results from direct temperature measurements of the tunnel type dryer, with comprehensive details highlighted in Table 1. The temperature changes were recorded every 30 minutes between 08:00 to 15:30 GMT+7.

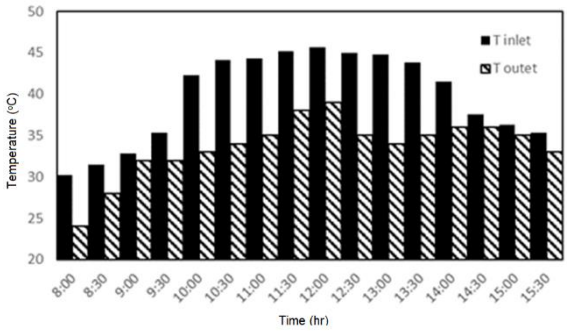

Figure 4: Inlet and outlet (experimental) temperatures on February 9, 2021.

Table 1: Tunnel-type dryer temperature data from experimental

Time (GMT+7)	T_{finlet} (ºC)	T_1 (ºC)	T_2 (ºC)	T_3 (ºC)	T_{foutet} (ºC)	$T\infty$ (ºC)
08:00	30.2	23.5	23.3	22.9	24	26
08:30	31.5	23.9	23.5	23.8	28	28
09:00	32.8	24	24.2	24.3	32	29

09:30	35.3	26.9	27.1	27.9	32	30
10:00	42.3	36.1	35.6	35.2	33	30
10:30	44.1	50.4	49.8	50.0	34	33
11:00	44.3	51.5	51.3	51.2	35	32
11:30	45.2	52.5	53.1	52.3	38	33
12:00	45.7	53.2	52.2	51.5	39	32
12:30	45.0	53	52.2	51.1	35	30
13:00	44.8	52.1	52.5	51.4	34	32
13:30	43.8	46.2	45.9	45.1	35	31
14:00	41.5	46.9	44.2	44.0	36	30
14:30	37.6	42.3	41.3	40.7	36	30
15:00	36.3	40.3	38.3	37.0	35	31
15:30	35.3	36.3	36.4	35.8	33	30

At the beginning of the measurement, the temperature increased from 08:00 to 12:00 GMT+7. Subsequently, a continuous decrease was reported from 12:30-15:30 GMT+7. This is in accordance with Harun et al.'s (2016) research stating that sunlight intensity between morning and noon is used to dry cocoa and by evening, the performance is analyzed [15].

3.2. Computing Results

Figure 5 shows the actual data of the input temperature distribution of the tunnel-type dryer. Although an orange color gradation dominated the drying floor plate between 12:00-14:00 GMT+7, a light green appearance occurred due to relatively low internal temperature.

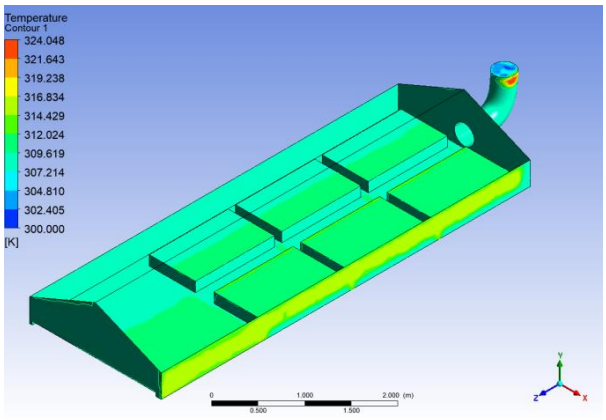

(a)

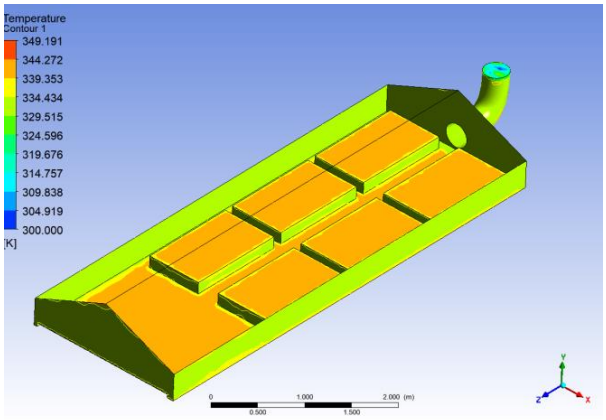

(b)

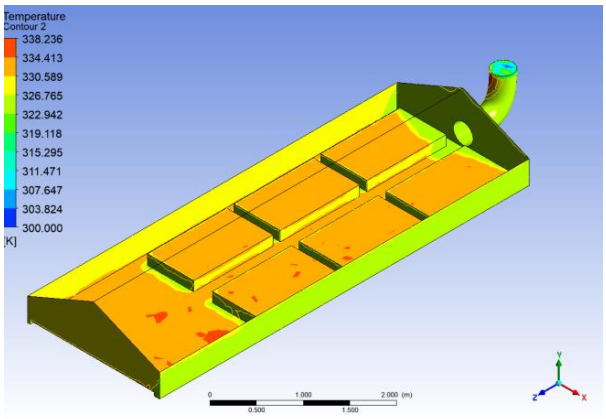

(c)

Figure 5: Temperature distribution contour at: (a) 08:00; (b) 12:00; and (c) 14.00 GMT+7.

The floor temperature appeared relatively higher compared to other areas. Therefore, it is best used to dry the material using direct contact with sunlight. The roof in this simulation was introduced to semi-transparent radiation. Table 2 summarizes the calculated temperature values, as indicated by the color gradation.

Table 2: Computational temperature values for tunnel-type dryers

Time (GMT+7)	T_{finlet} (ºC)	T roof (ºC)	T floor(ºC)	T Wall(ºC)	T_{foutet} (ºC)
8:00	34.4	36.6	36.3	36.6	31.2
8:30	38.4	41.8	41.8	40.8	34.0
9:00	42.1	46.5	46.7	44.7	36.3
9:30	46.0	51.0	51.5	49.1	38.0
10:00	51.2	54.0	55.1	52.0	39.4
10:30	54.8	59.6	61.2	57.2	42.0
11:00	55.8	60.4	62.4	57.6	43.3
11:30	58.6	62.9	65.2	59.7	44.1
12:00	58.8	63.0	65.6	59.3	43.4
12:30	58.0	61.2	64.0	57.2	43.2
13:00	58.4	62.8	65.5	59.3	43.1
13:30	56.6	60.7	63.1	57.6	43.0
14:00	52.5	56.3	57.7	54.0	40.4
14:30	49.9	56.3	57.8	53.9	41.4
15:00	48.5	54.7	55.7	52.7	40.3
15:30	46.4	50.7	51.1	48.8	38.6

Figure 2 shows the temperature contour in the outlet area from the computational simulation results. Several color gradations were observed due to the continuous temperature reading. Table 3 compares the outlet values from the temperature simulation and dryer measurements. The results showed an initial value of 30.2ºC in the inlet area at 08:00 GMT+7, which increased to a peak of 45.7ºC between 08:00 to 12:00 GMT+7, before dropping to 35.3ºC at 15:30 GMT+7.

The outlet area's experimental and simulated temperatures at 08:00 GMT+7were reportedly 24 and 28.7ºC, respectively. These two temperatures attained maximum values of 39ºC and 41.5ºC at 12:00 GMT+7, before dropping at 15:30 GMT+7 to 33 and 34.4ºC.

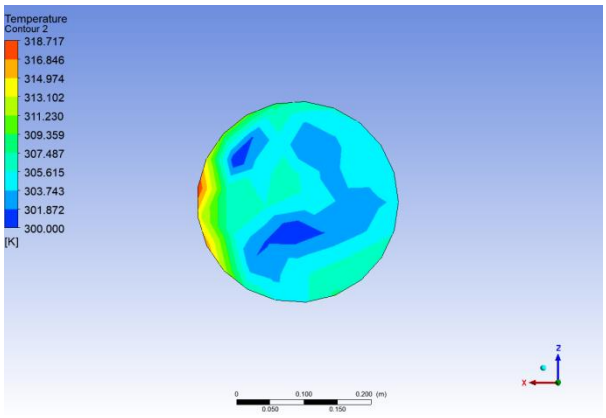

(a)

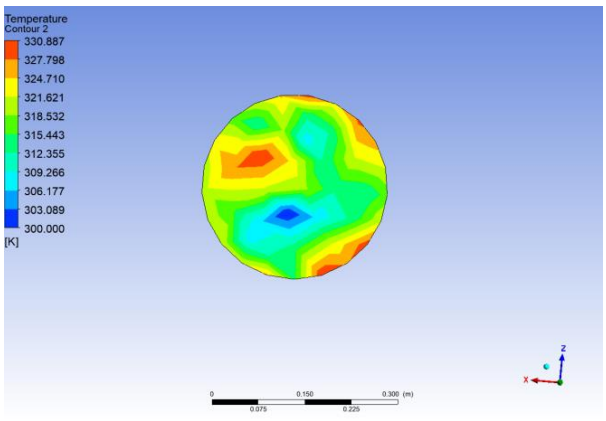

(b)

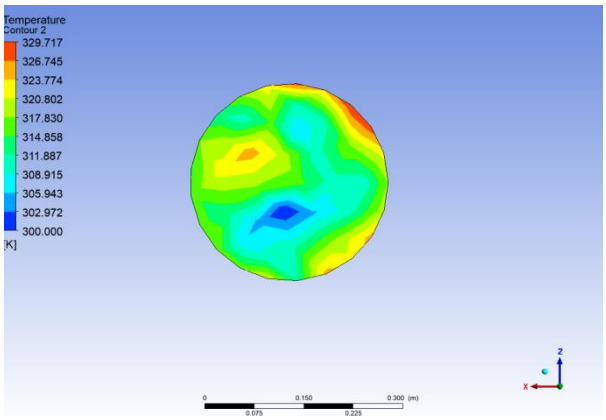

(c)

Figure 6: Outlet temperature contour at: (a) 08.00; (b) 12.00; and (c) 14.00 GMT+7.

Based on the experimental and simulation results, the maximum temperature occurred during the day at 12:00 GMT+7. This was in accordance with the increasing sunlight intensity time and the measurement results of solar intensity reported by Harun *et al.* (2016). The temperature value also reported increased as the cocoa dryer absorbed more heat [15]. Furthermore, the average temperature difference was approximately 1.25ºC higher in the computational simulations compared to the experimental results. This difference was attributed

to several uncontrolled parameters during the field data collection, such as unstable winds and irregular solar heat sources, measurement device deviations, etc.

Table 3: The comparison of experimental and computational temperature values in the outlet area of tunnel-type dryers

Time (GMT+7)	$T_{f\ inlet}$ (°C)	$T_{f\ outet}$ Eks. (°C)	$T_{f\ outet}$ Sim. (°C)
08:00	30.2	24	28.7
08:30	31.5	28	29.2
09:00	32.8	32	33.7
09:30	35.3	32	33.1
10:00	42.3	33	35.0
10:30	44.1	34	35.8
11:00	44.3	35	36.8
11:30	45.2	38	40.5
12:00	45.7	39	41.5
12:30	45.0	35	38.6
13:00	44.8	34	36.1
13:30	43.8	35	35.7
14:00	41.5	36	35.7
14:30	37.6	36	35.2
15:00	36.3	35	35.1
15:30	35.3	33	34.4

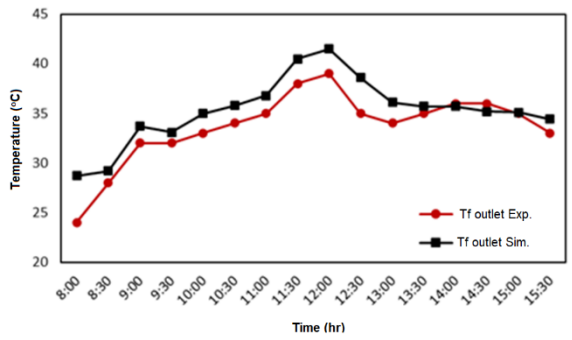

Figure 7: Comparison of outlet temperature values from experimental data with computational simulation data.

Figure 8 shows the results of the airflow pattern in the tunnel-type drying room at 08:00, 12:00, and 14:00 GMT+7 using CFD. Based on the illustration, the airflow appeared slightly intense on the lower side of the drying chamber. This condition is necessary to reduce the moisture content of the sample material.

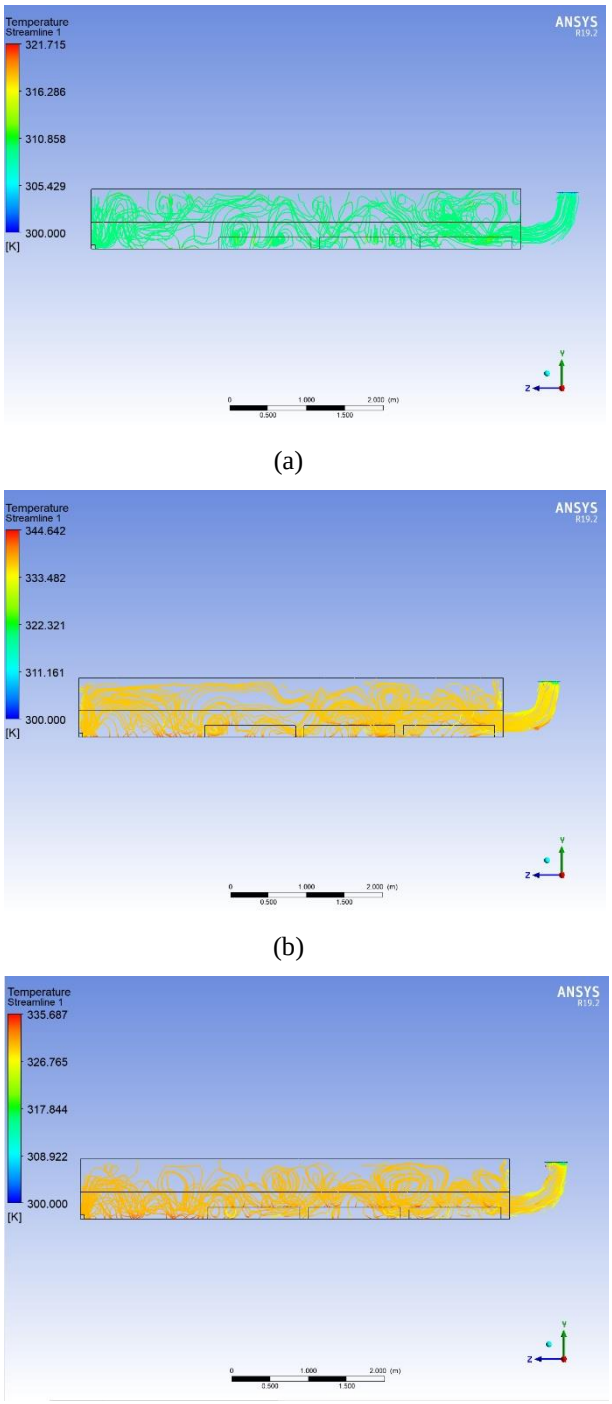

Figure 8: The pattern of airflow in the drying chamber at: (a) 08.00; (b) 12.00; and (c) 14.00 GMT+7.

Furthermore, the changes in color gradation were observed at 08.00, 12.00, and 14.00 GMT+7. The inlet airflow resulted in turbulence which helped to facilitate the drying process. This simulation was carried out without any load or drying sample, and the airflow was not turbulent. The use of sun-dried objects is expected to generate greater turbulence.

Consequently, the k-ε model is a powerful tool in analyzing the air velocity distribution pattern in the drying chamber, while the momentum equation triggers the actual simulation. Both conduction and convection (natural and forced) exchanges are formed in the drying system. Natural convection occurs in the absence of wind, which enables turbine rotation. Meanwhile, forced convection employs the device-generated wind to rotate the ventilator, enabling air to flow into the turbine ventilator and leave through the outlet.

Liquid air has the capacity to migrate from one place to another. It is categorized into various types, such as steady and transient [22]. The CFD method is also used to evaluate the fluid movement in a system based on computer software applications. This approach helps predict and analyze the fluid flow and heat transfer simulations [23]. One of its advantages is the provision of a broader understanding of the fluid flow distribution and heat transfer [24].

4. Conclusion

Based on the experiments and computational analysis results, the following conclusions were derived: The tunnel-type dryer experiences minimum temperature distribution at 08:00 GMT+7, with inlet and outlet temperatures of 30.2 and 24ºC, respectively. Meanwhile, the maximum inlet and outlet temperature distribution occurred at 12: 00 GMT+7, with values of 45.7 and 39ºC. Weather conditions and time mainly influenced these high and low circumstances. The computational simulations showed the lowest temperature distribution, similar to the experimental data at 08:00. The outlet temperature was at 28.7ºC, but attained the maximum value of 41.5ºC at 12:00 GMT+7. Furthermore, the computational and experimental value comparison did not vary extensively but obtained an average value of 1.25ºC. This indicates computational values serve as a comparison to obtain accurate results. The airflow into the drying chamber was simulated using CFD method. In addition, the generated results showed adequate airflow turbulence covering the entire drying chamber. This parameter has the capacity to reduce the water content of a drying sample significantly. Therefore, the tunnel-type dryer is suitable for post-harvest materials during agricultural, forestry, and marine applications.

Acknowledgments

The author is grateful to the Ministry of Education and Culture, DIKTI - Directorate of Research and Community Service and Institute for Research and Community Service (LPPM) Syiah Kuala University for the grants in funding this research.

Reference

[1] A. Fudholi, A. Ridwan, R. Yendra, A.P. Desvina, Hartono, M.K.B.M. Ali, T. Suyono, K. Sopian, “Solar Drying Technology in Indonesia: an Overview”, *International Journal of Power Electronics and Drive System (IJPEDS)*, Vol. 9, No. 4, pp.1804-1813, 2018.

[2] R. Saidur, G. BoroumandJazi, S. Mekhlif, M. Jameel, “Exergy analysis of solar energy applications”, *Renewable and Sustainable Energy Reviews*, Vol. 16, pp.350– 356, 2012.

[3] A.Z. Hafez, A. Soliman, K.A. El-Metwally, I.M. Ismaila, “Tilt and azimuth angles in solar energy applications–A review”, *Renewable and Sustainable Energy Reviews*, Vol. 77, pp.147–168, 2017.

[4] D. Harun, Zulfadhli, Akhyar, “The experimental performance of the semi-cylindrical type of solar concentrator collector on the addition of heat storage material”, *IOP Conference Series: Materials Science and Engineering*, Vol. 602, No. 1, 012082, 2019.

[5] D. Harun, M.I. Maulana, Akhyar, “The effect of solar water heater performance by variation of the plate-shaped”, *IOP Conference Series: Materials Science and Engineering*, Vol. 602, No. 1, 012081, 2019.

[6] D. Harun, M.I. Maulana, Akhyar, “Increase the heating capacity of solar water heaters through two conditions of placing paraffin in copper tubes”, *IOP Conference Series: Materials Science and Engineering*, Vol. 523, No. 1, 012077, 2019.

[7] G. Alva, L. Liu, X. Huang, G. Fang, “Thermal energy storage materials and systems for solar energy applications”, *Renewable and Sustainable Energy Reviews*, Vol. 68, 693–706, 2017.

[8] G. Pikraa, A. Salima, B. Prawaraa, A.J. Purwantoa, T. Admonoa, Z. Eddy, “Development of small scale concentrated solar power plant using organic Rankine cycle for isolated region in Indonesia”, *Energy Procedia*, Vol. 32, pp.122 – 128, 2013.

[9] Dinas Kelautan dan Perikanan Aceh, “Buku Statistik Tangkap 2016”, Banda Aceh, 2016.

[10] M.I. Maulana, “Penggunaan Energi Bahan Bakar Untuk Pengeringan Ikan Asin/Keumamah”, *Mekanika*, Vol. 8, No. 2, pp. 178-179, 2010.

[11] E. Arruda, J. Façanha, L. Pires, A. Assis, M. Barrozo, “Conventional and modified rotary dryer: Comparison of performance in fertilizer drying”, *Chemical Engineering and Processing: Process Intensification*, Vol. 48, No. 9, pp.1414-1418, 2009.

[12] Available online at: Schematic-diagram-of-the-drying-tower-and-air-distribution-ring.png [Accessed 27 December 2021]

[13] Available online at: screw conveyor dryer - Penelusuran Google [Accessed 27 December 2021]
[14] M. Eltawil, M. Azam, A. Alghannam, "Solar PV powered mixed-mode tunnel dryer for drying potato chips", *Renewable Energy*, Vol. 116, pp.594-605. 2018.
[15] D. Harun, H. Akhyar, R. Thai, "Performance Investigation and Development of Solar Dryer Tunnel Type Apparatus of Cocoa", *Proceedings of International Conference on Engineering and Science for Research and Development (ICESReD) 2016*, October 25-26, 2016, Banda Aceh, Indonesia, pp. 1-6, 2016.
[16] T. Norton, D.W. Sun, "Computational fluid dynamics (CFD) – an effective and efficient design and analysis tool for the food industry: a review", *Trends in Food Science and Technology*, Vol. 17 pp.600–620. 2006.
[17] Y. Amanlou, A. Zomorodian, "Applying CFD for designing a new fruit cabinet dryer", *Journal of Food Engineering*, Vol. 101, pp. 8–15, 2010.
[18] A.M. Foster, M. Madge, J.A. Evans, "The use of CFD to improve the performance of a chilled multi-deck retail display cabinet", *International Journal of Refrigeration*, Vol. 28, pp. 698–705, 2005.
[19] D.P. Margaris, A.G. Ghiaus, "Dried product quality improvement by airflow manipulation in tray dryers", *Journal of Food Engineering*, Vol. 75, pp.542–550, 2006.
[20] O. Yongsan, I.A. Badruddin, Z.A. Zainal, P.A.A. Narayana, "Airflow analysis in an air conditioning room", *Building and Environment*, Vol. 42, pp.1531–1537, 2007.
[21] D. Harun, M.I. Maulana, H. Akhyar, "Experimental investigation on open sun-drying and solar drying system of bilimbi", *2016 6th International Annual Engineering Seminar (InAES)*, pp. 271-275, 2016.
[22] R.M. Olson, S.J. Wright, "Dasar-Dasar Mekanika Fluida Teknik", *PT Gramedia Pustaka Utama*, Jakarta. 1990.
[23] H.K. Versteeg, W. Malalasekera, "An Introduction to Computational Fluid Dynamics the Finite Volume Method", *Longman Sc & Technical, Malaysia*, 1995.
[24] Al-Kindi, Hablinur, "Analisis CFD Aliran Udara Panas pada Pengering Tipe Rak dengan Sumber Energi gas Buang", *Jurnal Keteknikan Pertanian*, Vol. 3, No. 1, pp. 1-10, 2015.